

MHD Studies in JET Hybrid Plasmas with Electron Heating

P. Buratti¹, B. Alper², A. Becoulet³, P. Belo⁴, J. Bucalossi³, M. de Baar², P. de Vries², D. Frigione¹, C. Gormezano¹, E. Joffrin³, P. Smeulders¹ and JET EFDA contributors*

¹EURATOM-ENEA Association, C.R. Frascati, CP 65, 00044 Frascati, Italy. ²Euratom/UKAEA Fusion Association, Culham Science Centre, Abingdon. ³Association Euratom/CEA, Cadarache, France. ⁴Associação EURATOM/IST, Centro de Fusão Nuclear, 1049-001 Lisbon, Portugal, *see the Appendix of J.Pamela et al., Fusion Energy 2004 (Proc. 20th Int. Conf. Vilamoura, 2004) IAEA, Vienna (2004).

1. Introduction

The "hybrid" regime has emerged as a promising scenario from a number of tokamak experiments [1-4]. The distinguishing feature of this regime with respect to standard H-mode is the absence of strong sawtooth activity, which is achieved by current profile optimisation. Heating was dominated in most cases by neutral beam injection (NBI). Hybrid scenarios were developed at JET in 2004 with strong ion cyclotron resonance heating (ICRH) [5], which adds burning plasma physics issues like central electron heating and super-Alfvénic ions. Typical parameters were $B_T=3.2$ T, $3.8 \leq q_{95} \leq 5.5$, up to 10 MW of ICRH at 51 MHz with 4% H minority, normalized beta $\beta_N \leq 1.5$ (power limited), central temperatures $T_e \approx 10$ keV, $T_i \approx 6$ keV, central density $n_e \approx 3 \cdot 10^{19} \text{ m}^{-3}$. MHD studies on these experiments will be reported in this paper.

2. Overview of MHD activity

The significant portions of a typical spectrogram of magnetic signals are shown in fig. 1. Lines in the band above 500 kHz lie in the range of ellipticity-induced Alfvén eigenmodes (EAE) centered at the $q=1$ surface. Lines around 160 kHz correspond with toroidicity-induced Alfvén eigenmodes (TAE) at $q \approx 1.5$. The line at 21 kHz is a saturated $n=3$ neoclassical tearing mode (NTM). Last but not least, modes that cyclically flare-up below 10 kHz have $n=1$ toroidal number and internal kink-like structure

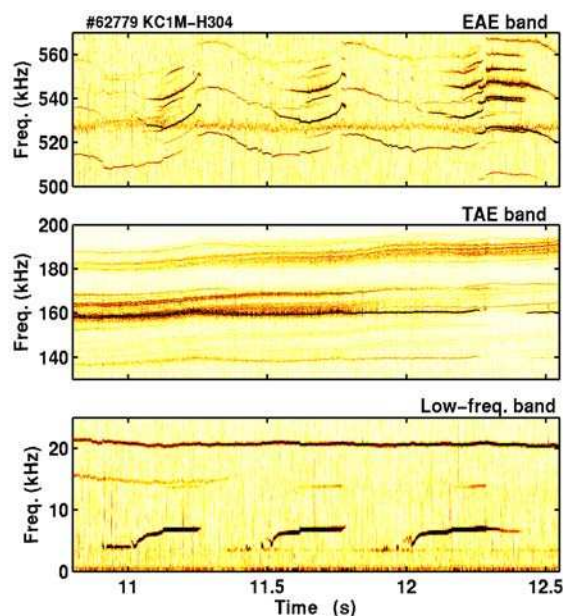


Figure 1. Spectrogram of a magnetic signal in a hybrid JET discharge with $B=3.2$ T, $I=2.3$ MA, $P_{ICRH}=7.6$ MW, $P_{NBI}=7.8$ MW, $q_{95}=4.6$, $\beta_N=1.4$. Sampling rate=2 MHz, $nfft=8192$.

like sawtooth precursors; their time evolution is however very different (see sect. 4) and for this reason these modes will be referred to in the following as "slow sawteeth".

3. NTMs, fishbones and comparison with NBI-heated hybrid regimes.

MHD activities of hybrid regimes with dominant NBI heating include NTMs and/or fishbones. Fig. 2a shows an example with two NTMs at 15 and 27 kHz, fishbones between 12 and 15 kHz, and $n=1$ activity of the slow sawtooth kind at 9 kHz. Changes of NTM rotation frequencies are due to type I ELMs. Fig. 2b shows the beginning of main heating in a discharge with strong ICRH. An isolated fishbone (a few in other similar pulses) with large frequency span occurs, and a NTM grows without any evident trigger event. Slow sawteeth like the ones shown in fig. 1 appear later. ELMs are of type III in all cases with strong ICRH [5] and have no visible effect on internal modes.

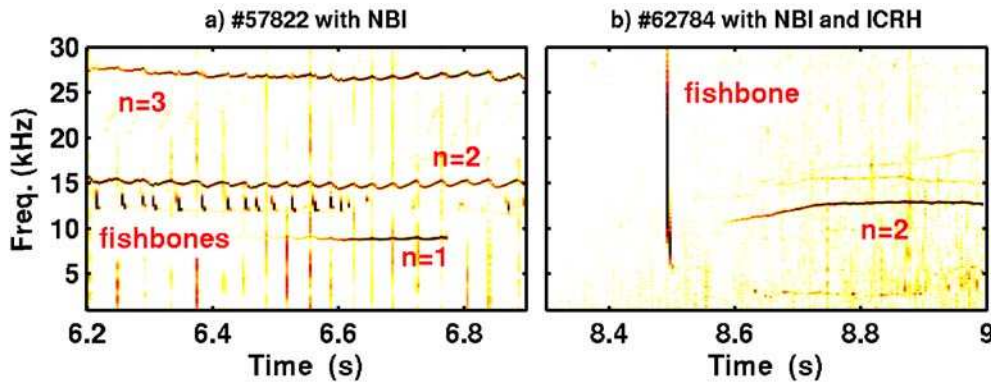


Figure 2. a) Magnetic activity in JET pulse 57822, $B=1.7$ T, $I_p=1.4$ MA, $P_{NBI}=8$ MW, main heating start at $t=4$ s. b) Pulse 62784, $B=3.2$ T, $I_p=2.3$ MA, $P_{NBI}=8$ MW, $P_{ICRH}=7$ MW, main heating start at $t=8$ s.

Hybrid discharges with strong ICRH have in most cases an $n=2$ dominant NTM and weaker ones with higher n . In a few cases (see fig. 1) a single $n=3$ NTM can be found. The typical T_e profile displacement due to NTMs is less than 1 cm at $\beta_N=1.5$; the associated island full width can be estimated as $w=3.8$ cm [6], which should have negligible global effects. Higher β_N values could not be explored due to power restrictions, however the island saturation amplitude should roughly scale linearly with β_N . Tolerable NTM amplitudes have been reported up to $\beta_N \approx 3$ in NBI discharges in DIII-D and JET [3, 7]. Fishbones usually occur only at the beginning of main heating; they can persist during main heating either at lower ICRH power ($P_{ICRH} < 5$ MW) or in discharges that revert to normal sawtooth activity.

4. The slow sawtooth

The spatial structure of $n=1$ oscillations can be extracted by frequency-selective coherence analysis between magnetic signals and local temperature oscillations from ECE. Fig. 3 shows the profile of $n=1$ temperature oscillations (δT_e) together with q -profile from MSE

nearest in time. Both profiles are projected onto the equatorial plane; δT_e data have a gap since the ECE sightline is below the equatorial plane. T_e oscillations are clearly localised in the central region, where $q \approx 1$. Their profile is of the internal kink-type, with phase inversion at the foot. The maximum peak-to-peak displacement is $\Delta = \delta T_e / |dT_e/dR| \approx 2$ cm. These characteristics are in common with sawtooth precursors, but there are two striking differences. First, $n=1$ oscillations are long-lasting (from 250 to 500 ms, see fig. 4), while ordinary sawtooth precursors are much faster; second, the effect on temperature profiles is a mild erosion [8], very different from the flattening produced by normal sawteeth.

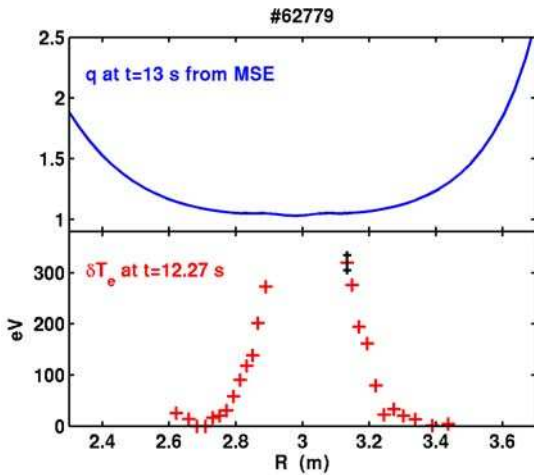


Figure 3. q -profile and $n=1$ temperature oscillations from ECE signals. The black segment represents a typical error bar.

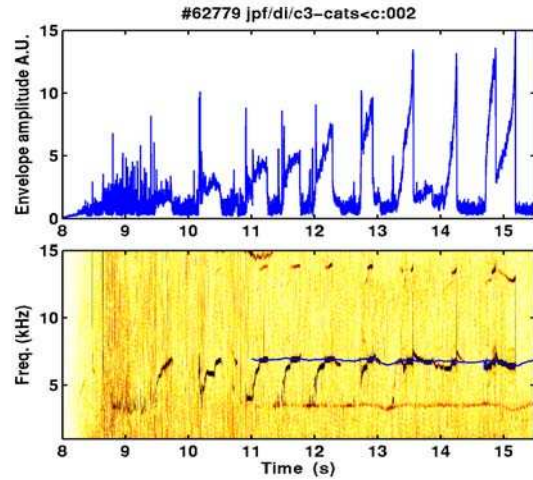


Figure 4. Envelope and spectrogram of $n=1$ magnetic oscillations. The blue line shows the NTM rotation frequency.

Amplitude and frequency evolution of $n=1$ oscillations are shown in fig. 4. The first cycles feature algebraic growth followed by saturation and damping. After $t=13$ s, exponential or super-exponential growth followed by a sharp drop is observed. These variations are associated with progressive peaking of the current profile. Frequency of $n=1$ modes tends to track the NTM rotation frequency ($f_{ROT} = f_{NTM} / n_{NTM}$, shown by the blue line on the spectrogram in fig. 4) as the amplitude grows.

5. Toroidal Alfvén Eigenmodes

The sharp amplitude drop occurring at the end of $n=1$ cycles with exponential or super-exponential growth is accompanied by a burst of high-frequency activity. Spectral analysis reveals that this activity is a flash of TAE modes (fig. 5). No such event is observed at the end of $n=1$ cycles with saturation or algebraic growth. The TAE flash is likely to be due to migration of fast particles from the central region to the $q \approx 1.5$ region; this indicates that slow sawteeth in the exponential form start affecting fast particles confinement.

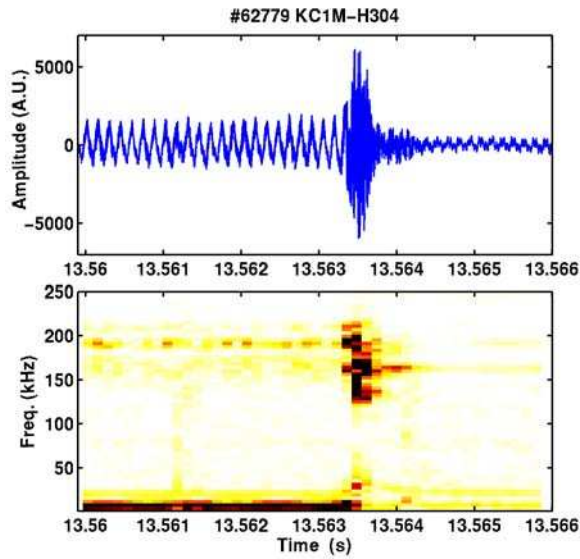


Figure 5. Magnetic signal and spectrogram at the end of an exponential $n=1$ cycle. The high-frequency burst is in the TAE region 150-200 kHz.

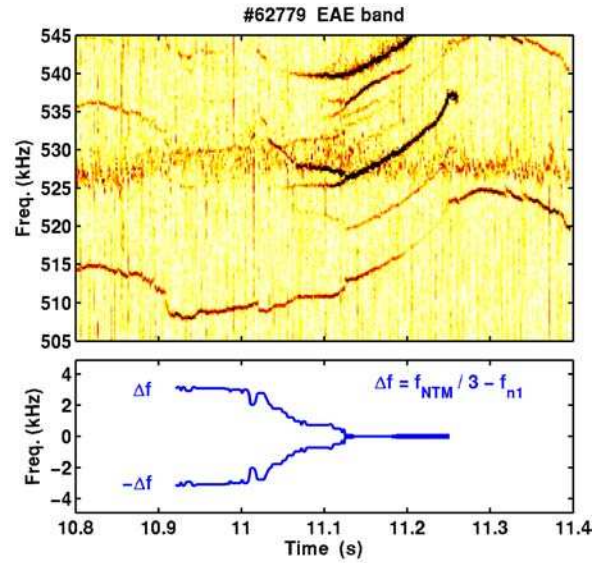


Figure 6. Close-up of the EAE band and difference between $n=1$ and NTM rotation frequencies. The latter is only shown when the $n=1$ mode has detectable amplitude.

6. Ellipticity-induced Alfvén Eigenmodes

The EAE spectral region changes during $n=1$ cycles. Slow variations of pre-existing lines can be attributed to local changes of density or q -profiles [9]. More interestingly, new lines appear, whose frequencies coalesce as the $n=1$ frequency tracks the NTM frequency (fig.6); this indicates that non-linear interactions between EAEs and $n=1$ mode are taking place.

7. Discussion

Hybrid-regime plasmas with strong central electron heating by ICRH, which are in some respects representative of burning plasmas, feature Alfvén eigenmodes, NTMs and $n=1/m=1$ activity. The latter is in a very unusual form, the slow sawtooth; its macroscopic effects are negligible provided that the current profile remains broad enough. Some evidence of non-linear interactions between $n=1$ and EAE modes has been found.

References

- [1] E. Joffrin et al., 20th Fusion Energy Conf., EX/4.2, to be published on Nucl. Fusion.
- [2] A.C.C. Sips et al., Plasma Phys. Contr. Fusion **44** (2002) B69.
- [3] T.C. Luce et al., Phys. Plasmas **11** (2004) 2627.
- [4] A. Isayama et al., Nucl. Fusion **43** (2003) 1272.
- [5] C. Gormezano et al., Plasma Phys. Contr. Fusion **46** (2004) B345.
- [6] R. Fitzpatrick, Phys. Plasmas **2** (1995) 825.
- [7] P. Belo et al., Proc. 31st EPS Conf. on Plasma Physics, London 2004, P1-170.
- [8] P. Buratti et al., Proc. 31st EPS Conf. on Plasma Physics, London 2004, P1-165.
- [9] G.J. Kramer et al., Nucl. Fusion **41** (2001) 1135.